

Tool wear and surface roughness analysis in hard turning of AISI 4340 steel with coated carbide inserts

M. Zulfiqar¹, A.S. Jamali¹, S. Hussain² 

¹Quaid-e-Awam University of Engineering, Science and Technology, Nawabshah, Sindh, Pakistan

²Indus University, Karachi, Pakistan

✉ muradzulfiqar@gmail.com

ABSTRACT

The performance of CVD-coated carbide inserts (TiCN/Al₂O₃) in hard turning AISI 4340 steel at cutting speeds of 60, 95, 180, and 250 m/min, under both dry and wet conditions are investigated. The goals were to evaluate tool wear, surface roughness, and wear mechanisms over different machining conditions. Surface roughness Ra value was noticed, and it dropped to Ra = 0.30 μm at 180 m/min but increased at 250 m/min due to vibration, edge instability, and wear. Flank wear rose with cutting speed: 186 μm at 60 m/min, 265 μm at 180 m/min, 542 μm at 250 m/min (dry), and 692 μm (wet), exceeding ISO tool life (VB = 300 μm) due to edge breakage, flaking, and adhesion. The examination of the tool surface by SEM and EDS revealed abrasion and slight coating delamination at low speeds, adhesion and oxidation at intermediate speeds, and catastrophic tool failure at high speeds.

KEYWORDS

AISI 4340 steel • CVD coated insert • hard turning • surface roughness

Citation: Zulfiqar M, Jamali AS, Hussain S. Tool wear and surface roughness analysis in hard turning of AISI 4340 steel with coated carbide inserts. *Materials Physics and Mechanics*. 2026;54(1): 101–117.

http://dx.doi.org/10.18149/MPM.5412026_10

Introduction

AISI 4340 is a medium carbon low alloy steel, widely known for its good tensile strength. It is commonly used in making shafts, gears, screws and heavy-duty studs. Because of its properties, especially after hardening, it is applied in aerospace, automotive and defense industries for critical components where toughness and reliability are very important [1]. The alloying elements like chromium, nickel and molybdenum improve their hardenability and strength. But the same factors that give high performance also make machining very difficult, especially when hardness is above 45 HRC (hardness Rockwell C). Under dry or severe cutting conditions this problem gets even worse. In machining, the main difficulties are fast tool wear, high cutting temperature, and heavy friction at the chip–tool interface. These lead to thermal instability, dimensional inaccuracy, and poor surface quality, which eventually affect productivity and cost [2,3]. Even with conventional coolant, the wear cannot be fully eliminated because cutting fluid does not always reach the chip–tool zone effectively at high speed and hardness [4]. Hardened AISI 4340 has a tempered martensitic microstructure that strongly resists plastic deformation. This makes it fall under difficult-to-machine materials since machining produces high forces and high wear, as reported by Boztepe et al. [5]. The presence of hard carbides in tempered martensite accelerates abrasive wear and reduces tool life.



Selvaraj [6] showed the adhesive and abrasive wear on the cutting tool at higher cutting speeds negatively affect the surface finish of the workpiece. Darwish [7] mentioned that tool wear is a key reason for poor surface finish, inaccuracies and shorter tool life. Minouiz et al. [8] noted adhesion, abrasion and edge rounding as main wear mechanisms for PVD-coated tools, while for CVD (chemical vapor deposition) coated tools built-up edge (BUE) and chipping were dominant during continuous cutting at high speed. Calaph et al. [9] observed that speed, feed and depth of cut have significant influence on flank wear in CNC (computer numerical control) turning of EN8 steel. Šramhauser et al. [10] also showed that coating thickness and structure matter a lot, thinner Al_2O_3 (aluminium oxide) improved chip flow and heat transfer while TiN-coated tools gave surface roughness of $0.76 \mu\text{m}$.

Furthermore, Bag et al. [11] studied hardened AISI 4340 and found cutting speed as the most dominant factor (66.06 %) influencing flank wear. They reported that increasing speed from 80 to 260 m/min caused rubbing due to high temperature and pressure, leading to thermal softening of the cutting edge. Butt et al. [12] observed similar wear trends for turning of 45 HRC AISI 4340 using TiCN (titanium carbonitride)/ Al_2O_3 /TiN carbide tools at speeds 50–200 m/min and feeds 0.051–0.101 mm/rev. Kishore et al. [13] further showed that the temperature resulting from the tool-workpiece rubbing causes larger surface wear and defects. The tool flank rubs against the surface of material and adhesive wear, abrasion combined with heat is produced from contact. Hurtasenko et al. [14] associated very high shear zone temperatures with adhesive, diffusion, and brittle fracture type wear. Hassan et al. [15] reported crater wear as the main form in machining DC53 steel hardened to 40 HRC. Likewise, Santos et al. [16] observed adhesion–abrasion wear during dry micro-milling of AISI D2. With development of coatings and improved tool geometry, wear has been reduced. Ahmed et al. [17] showed that TiAlN coating increased tool life, while Jouini et al. [18] found that Al_2O_3 /TiCN coating improved surface quality at high speeds on AISI 4340. Silva et al. [19] reported that coated tools had better thermal stability, while Çakan et al. [20] noted TiSiN+ Al_2O_3 +TiN multilayers gave better results when turning AISI D2. Rashid et al. [21] studied hard turning of AISI 4340 with a CBN insert and obtained very low surface roughness ($0.45 \mu\text{m}$). They also concluded that lower feed improves finish but increases wear, showing the trade-off between tool life and surface quality. More improvement was also noted with multilayer coatings. Kumar et al. [22] reported over 15 times higher tool life in dry drilling of AISI D2, and Hamadi et al. [23] confirmed better tool life for coated inserts while machining AISI 4140. Dry high-speed machining is considered cost-effective and environmentally friendly [24]. But at very high speeds, cutting force, plastic deformation and surface damage increase, which accelerates tool wear and reduces quality [25,26].

Although many studies are done on tool wear and surface roughness separately, only few looked at their direct relationship under dry and wet machining with coated carbide tools at high speeds. Also, the exact wear mechanisms that affect surface finish are still not clear. From the literature, it can be seen that little work is reported on Al_2O_3 /TiCN multilayer CVD-coated carbide tools in high-speed hard turning of hardened AISI 4340 steel. Since high-speed machining is important for achieving good surface finish, this gap is critical. Therefore, the present study investigates tool wear and surface roughness of hardened AISI 4340 steel at different cutting speeds. SEM (scanning electron microscopy) and EDS (energy dispersive spectroscopy) analysis are used to identify the dominant wear

mechanisms. This work contributes to better understanding of machinability of AISI 4340 steel and offers practical guidance for optimizing cutting conditions, monitoring tool wear, and improving surface finish in hard turning.

Materials and Methods

Material and heat treatment

Commercial AISI 4340 steel rods, sourced from Peoples Steel Mills in Pakistan, were used in this study. The material, in its as-received state, had a hardness of nearly 30 HRC. In order to bring the hardness level suitable for hard turning, the rods were heat treated. The treatment involved austenitizing at 850 °C for 120 min in an RJX-45 box furnace, then quenching in HJ-20 oil to near room temperature. and subsequently tempered at 480 °C for 120 min. The purpose of this tempering step was to relieve internal stresses, lower brittleness, and at the same time enhance toughness while still keeping the hardness at a high level. The final hardness, checked with an Insize Rockwell tester (ASTM E18) (Fig. 1(b)), was found to be around 55 ± 1 HRC. The chemical composition was determined using a Spectrolab M9 spectrometer shown in Fig. 1(a), while the microstructure was observed with a Versamet 2 metallurgical microscope. Prior to machining tests, the outer layer of the heat-treated rods was lightly cut to remove any surface inconsistencies. For each experimental run, a cutting length of 120 mm was used. Every set of machining parameters was repeated three times, giving a total cutting distance of 360 mm for each condition. The average values from the three repetitions were taken for further analysis.

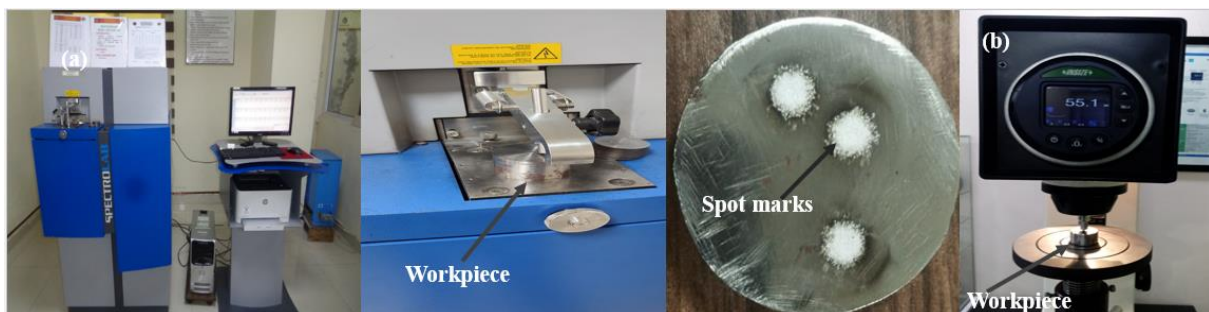


Fig. 1. Spectrometric analyses (a), hardness tester (b)

Experimental setup

Turning experiments were conducted utilizing a Goodway CGL-2 CNC lathe equipped with a FANUC Oi-TF control system shown in Fig. 2(a). The tool-workpiece configuration is depicted in Fig. 2(b), illustrating the hard turning of the heat-treated AISI 4340 steel. For wet machining trials at 250 m/min, a commercial mineral based cutting oil (Arab Lube, diluted at 1:20 with water) was applied as a conventional flood coolant, and was used exclusively at a cutting speed of 250 m/min as depicted in Fig. 2(c) The coolant was directed at the tool–chip interface through an external nozzle to evaluate its effectiveness at high-speed cutting conditions. Cutting experiments were carried out at four cutting speeds of 60, 95, 180, and 250 m/min, while the feed rate and depth of cut were kept constant throughout the study at 0.1 mm/rev and 0.5 mm, respectively. This

selective use was intended to compare dry and wet machining under maximum thermal load conditions, while all other trials were conducted dry. The experimental design is comprehensively detailed in Table 1.



Fig. 2. Experimental setup showing (a) CNC lathe, (b) tool and workpiece, hard turning, (c) wet cutting with coolant

Table 1. Workpiece and setup specifications

Parameters	Details / Specifications
Material	AISI 4340 Steel
Workpiece length, mm	200
Machining length, mm	120
Workpiece diameter, mm	30
Workpiece hardness, HRC	55 ± 1
Tooling	Mitsubishi CVD-coated carbide inserts (CNMG 120404)
Insert coating	CVD multi-layer coating of TiCN and Al ₂ O ₃
Tool nose radius, mm	0.4
Tool holder	PCLNR 2020K12
Machine	Goodway CGL-2 CNC Lathe with FANUC Oi-TF control
Cutting speeds, m/min	60, 95, 180, and 250
Machining environment	Dry conditions (low to high-speed machining); Cutting fluid for high-speed machining
Feed rate, mm/rev constant	0.1
Depth of cut, mm constant	0.5

Cutting tools

For the experimental machining trials, the cutting tool selected was a commercially available CVD coated carbide insert from Mitsubishi Materials [27]. This particular insert is characterized by a sophisticated multilayer coating system, primarily consisting of TiCN/Al₂O₃ layers, which is engineered to provide enhanced wear resistance and thermal stability during cutting. The geometry of the insert includes a defined tool nose radius of 0.4 mm, a feature critical for influencing surface finish and tool strength. A schematic representation detailing the insert's geometry can be found in Fig. 3. For mounting, the insert

was securely assembled onto a standard PCLNR 2020K12 style tool holder. Photographic evidence of the actual physical insert, along with its complete assembly onto the tool holder to show the final cutting geometry, is clearly provided in Fig. 4(a,b) respectively.

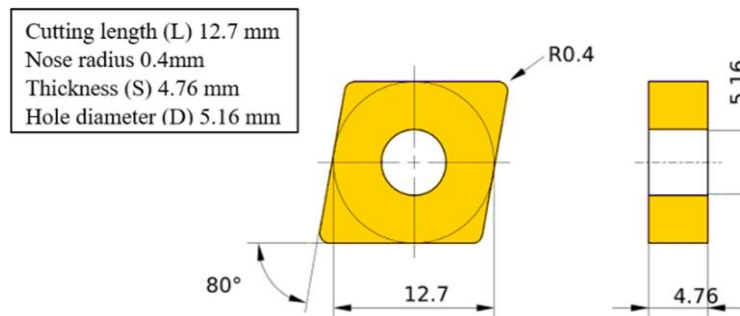


Fig. 3. Schematic of the selected CVD-coated carbide insert (CNMG 120404). Based on [27]

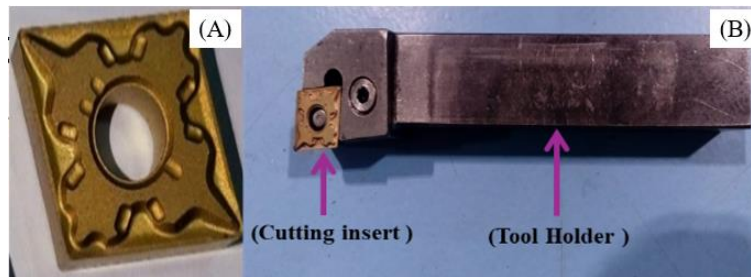


Fig. 4. (a) CVD-coated cutting insert; (b) insert mounted on PCLNR 2020K12 tool holder

Tool wear measurement

Flank wear (VB) was measured after each 120 mm cutting pass using a Dino-Lite Premier AM7013MT digital microscope, and the final values reported correspond to the tool condition after the third pass (total cutting length = 360 mm). An average flank wear criterion of $VB \geq 300 \mu\text{m}$ was adopted in accordance with ISO 3685 as the reference limit and measurement accuracy was ensured by calibrating the system with a certified stage micrometer before and during testing. For a more in-depth investigation into the fundamental mechanisms responsible for the wear, advanced characterization techniques

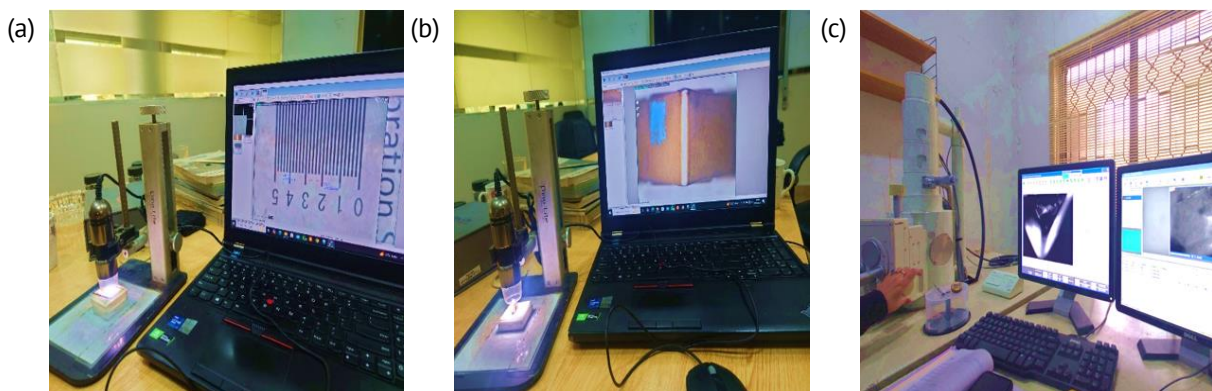


Fig. 5. Tool wear measurement and analysis setup: (a) calibration of Dino-Lite microscope; (b) flank wear measurement on tool edge; (c) SEM/EDS analysis of worn tools

were employed. This involved using SEM on a Jeol JSM 6380 unit, which provided high-magnification imagery of the wear scars and crater formation. Furthermore, energy dispersive X-ray spectroscopy (EDS) was performed with a JED-2300 detector attached to the SEM; this allowed for elemental analysis of the worn surfaces to identify diffusion and adhesion processes. The complete experimental arrangement used for these tool wear measurement and subsequent analysis procedures is visually detailed in Fig. 5.

Surface roughness measurement

Arithmetic average surface roughness R_a was measured in accordance with ISO 4287/4288 standards using a calibrated Mitutoyo SJ-310 tester, with a cutoff length of 0.8 mm, evaluation length of 4.0 mm, and probe speed of 0.5 mm/s. For each experimental condition, three roughness measurements were taken at distinct locations on the workpiece after each cut, and the mean value was used for analysis. The measurement setup is shown in Fig. 6. This integrated approach allowed direct correlation between tool wear progression and surface quality, while SEM/EDS analyses validated the underlying wear mechanisms.

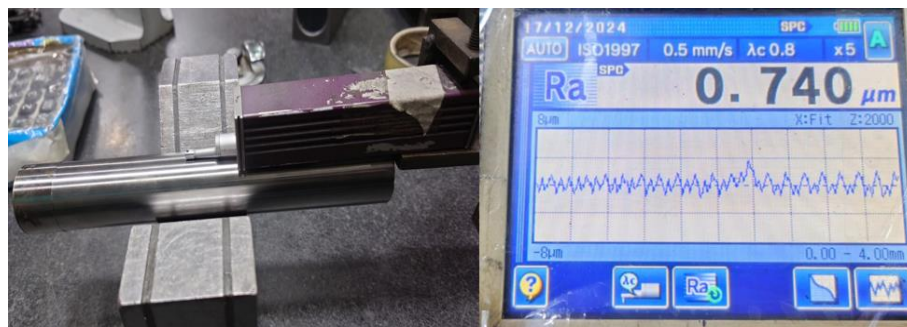


Fig. 6. Surface roughness measurement setup using Mitutoyo SJ-310 tester

Results and Discussion

Material characterization

The chemical composition of the heat-treated AISI 4340 steel is provided in Table 2. The measured values are consistent with the ASTM A29 standard range for AISI 4340. Chromium (Cr), nickel (Ni), and molybdenum (Mo) add hardness, strength, and ductility, while carbon (C) gives wear resistance by forming a carbide. The heat treatment applied provided a hardness level of 55 ± 1 HRC (ASTM E18), confirming suitability for hard turning.

The microstructure, given in Fig. 7, was prepared according to ASTM E3 and etched using 2 % Nital as per ASTM E407. A tempered martensitic matrix characteristic of quenched and tempered AISI 4340 steel was seen at a 400 × magnification. This structure provides high wear resistance by means of martensite and carbides, and toughness that causes high cutting forces and thermal stresses during cutting [15]. Understanding this microstructure is crucial for interpreting the machining behavior observed in the experiments, as it directly influences tool wear mechanisms and surface roughness outcomes.

Table 2. Chemical composition of heat-treated AISI 4340 steel (measured using Spectrolab M9)

Elements	C	Mn	Cr	Si	Ni	Mo	Fe
Wt. %	0.38	0.63	0.99	0.3	2.01	0.3	Balance

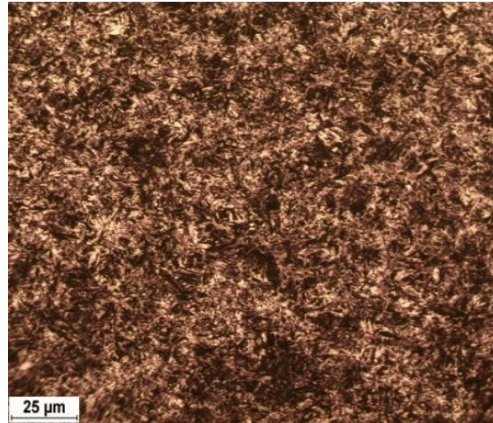


Fig. 7. Tempered martensitic microstructure of heat treated AISI 4340 steel

Surface roughness

The surface roughness (R_a) 0.931–1.069 μm with the cutting speed V of 60 m/min that corresponded to the three subsequent cuts (Fig. 8) was also characterized by a relatively high roughness. From 95 m/min, increasing the cutting velocity the surface roughness decreased to 0.657–0.877 μm (Fig. 9). At 180 m/min, even better results were achieved, showing R_a values of 0.303–0.612 μm (Fig. 10). Such a gradual decrease in R_a at higher speeds is considered to result from the shorter tool workpiece contact time and thermal

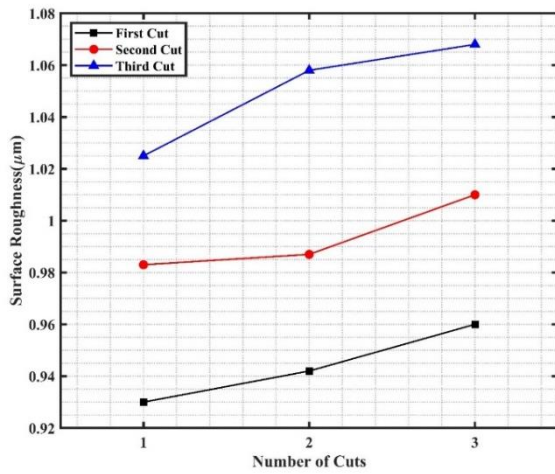


Fig. 8. Surface roughness at $V = 60$ m/min

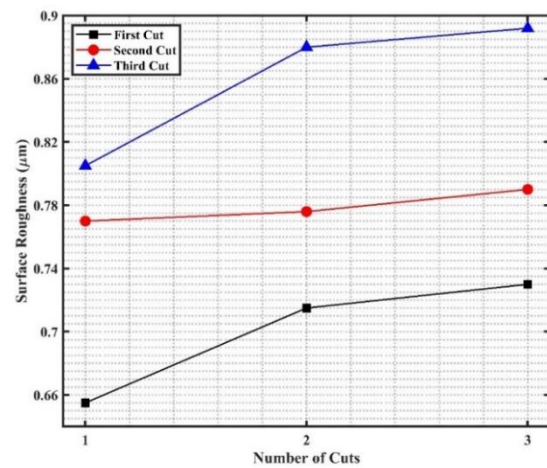


Fig. 9. Surface roughness at $V = 95$ m/min

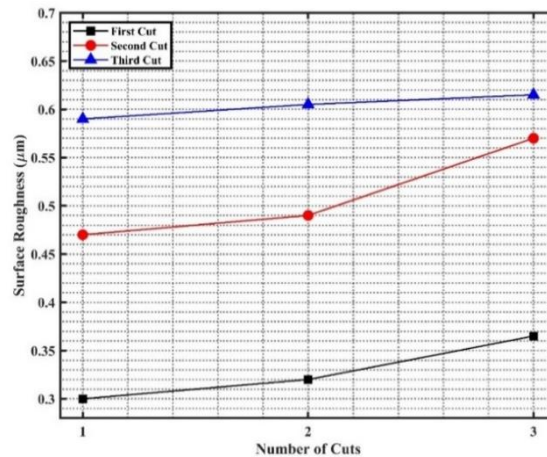


Fig. 10. Surface roughness at $V = 180$ m/min

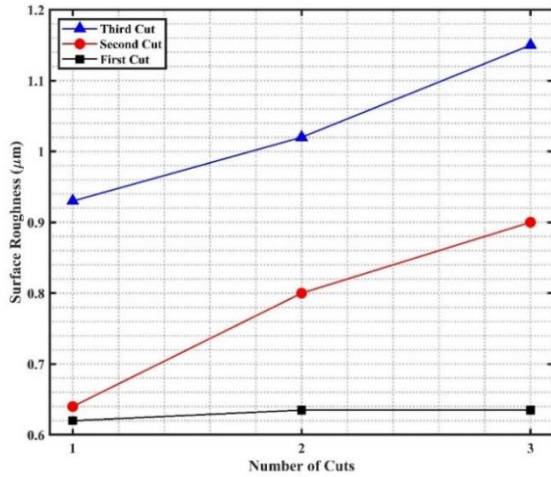


Fig. 11. Surface roughness at V = 250 m/min

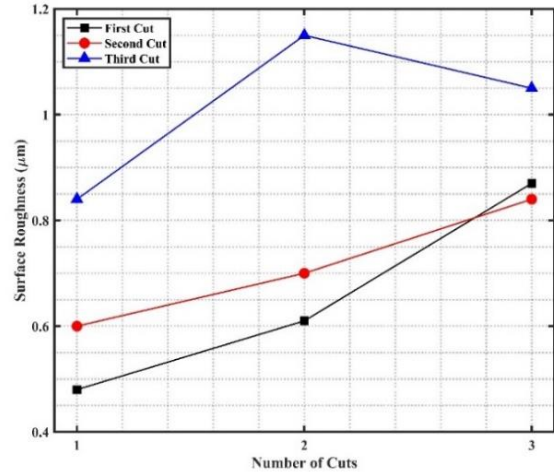


Fig. 12. Surface roughness at V = 50 m/min (wet)

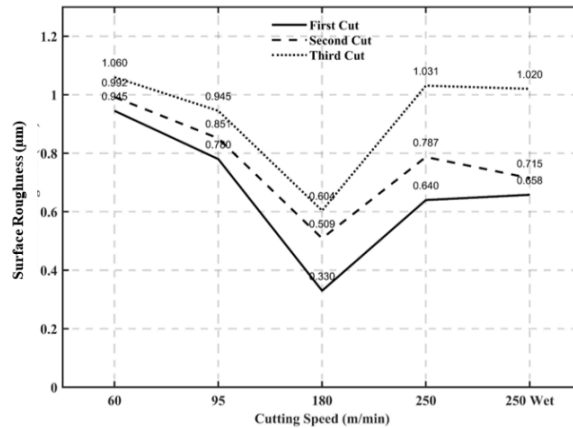


Fig. 13. Variation of surface roughness (R_a) with cutting speed for different numbers of cuts

softening of the workpiece material that enables smoother cutting. Similar trends have been reported in previous studies [28]. Surface roughness R_a was increased at 250 m/min (the maximum cutting speed) than at 180 m/min as depicted in Fig. 11. At higher cutting speeds, the cutting tool may suffer from extreme edge damage, such as flaking, notching or even catastrophic wear, which results in a blunt edge [18]. This can result in uneven cuts and differences in the texture of the surface. In addition, chatter and vibrations introduce oscillations at the tool edge, which cause the formation of an irregular surface pattern, and consequently an increase in the roughness [29].

Furthermore, for the highest speed of 250 m/min, surface roughness values became slightly better when wet cutting was performed (from 0.490 to 1.069 μm) than those for dry cutting, as presented in Fig. 12. It is noted that, despite the coolant application, R_a increased on the third cut, and the trend was different in comparison with the first cut at this speed. The uneven roughness pattern at high speeds, even during wet machining might be caused by vibration, instability, or sudden tool breakage and notching in the tool's cutting edge [30]. The general behavior is highlighted in Fig. 13, which collects R_a variation at all cutting speeds and conditions. The results show a U-shape, i.e., roughness decreases with increasing speed up to 180 m/min where the lowest surface roughness ($R_a \approx 0.30\text{--}0.61 \mu\text{m}$) was achieved, and increases again at 250 m/min. In wet cutting at

250 m/min, R_a values became better than for dry cutting but increased with respect to moderate cutting speeds (95–180 m/min). These findings confirm that moderate to high cutting speeds (95–180 m/min) provide the optimum balance between surface finish and machining stability, whereas excessively high speeds lead to deterioration despite the use of coolant, due to high cutting temperature and excessive tool wear [15].

Tool wear

Figure 14 depicts the flank wear (VB) evolution through several cuts at different cutting speeds. The wear measured from 186 μm at 60 m/min to 229 μm at 95 m/min, and 265 μm at 180 m/min. At 250 m/min, wear sharply increased to 542 μm under dry conditions, exceeding the ISO 3685 tool life standard ($V_b = 300 \mu\text{m}$). Under wet conditions at 250 m/min, wear reached 692 μm as depicted in Table 3 after final cut. Elevated temperatures in hard turning led to coolant evaporation, which failed to cool the tool, causing thermal softening and reduced wear resistance [31]. These results indicate that tool wear remains moderate up to 180 m/min but becomes significant beyond that, with catastrophic wear at 250 m/min.

Figure 15 illustrates the final flank wear value after the last cut, highlighting the sharp increase in wear, especially under wet conditions. Figure 16 digital microscopic pictures further illustrate wear progression at different cutting speeds, showing mild wear at 60 and 95 m/min, moderate wear at 180 m/min, and severe adhesion and localized chipping and indicating accelerated coating delamination with significant wear observed at 250 m/min. Under wet cutting conditions at the same cutting speed of 250 m/min, severe edge chipping, Flaking, coating delamination and were evident, this is due to high-speed machining of hardened steel generates high temperatures which result in failure of a tool [32].

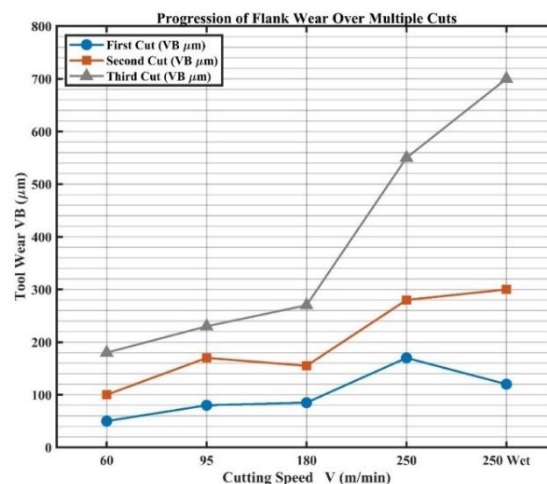


Fig. 14. Flank wear progression (μm) across first, second, and third cuts at different cutting speeds, including wet conditions

Table 3. Flank wear of CVD-coated tool at different cutting speeds after final cut

Speed, m/min	Flank wear, μm
60	186
95	229
180	265
250	542
250 (wet)	692

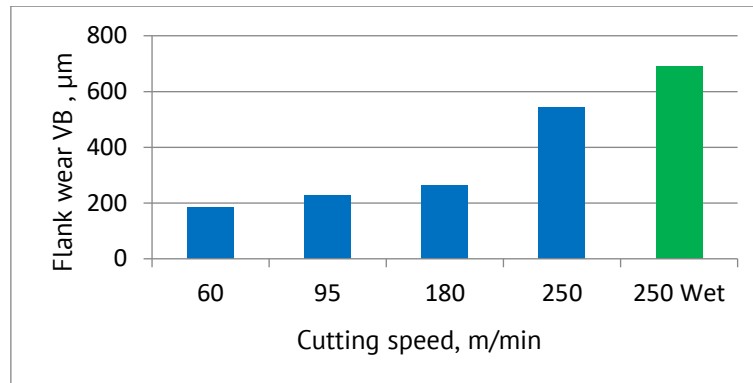


Fig. 15. Flank wear (VB) after final cut at different cutting speeds under dry and wet conditions

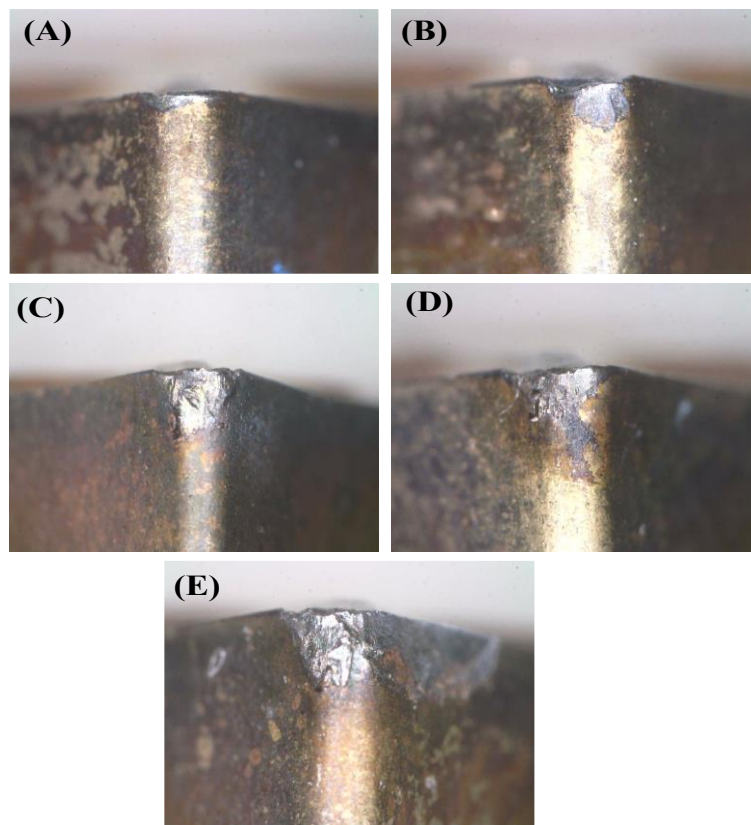


Fig. 16. Optical images of tool wear progression at cutting speeds: (a) 60 m/min; (b) 95 m/min; (c) 180 m/min; (d) 250 m/min (dry); (e) 250 m/min (wet)

SEM and EDS analysis of cutting tool

The EDS analysis of the fresh CVD-coated carbide insert, shown in Fig. 17 reveals the presence of carbon (C), oxygen (O), aluminum (Al), and titanium (Ti) supporting the multi-layer coating structure ($\text{TiCN}/\text{Al}_2\text{O}_3$) on the tool. Notably no tungsten (W) was noticed on the fresh tool surface, as the underlying substrate is fully covered by the CVD coating. This baseline composition provides a clear reference for interpreting element redistribution during machining.

The substantial tungsten content observed in the EDS analyses of worn tool surfaces (10–59 wt. % in Figs. 18–22) is attributed to the substrate material (W). As seen in the EDS analysis of the fresh insert (Fig. 17), no tungsten is detected on the unused tool due

to complete coverage by the multi-layer CVD coating. The presence of tungsten after cutting, particularly at higher cutting speeds, indicates local delamination of the coating, exposing the tungsten-rich substrate. Variations in tungsten content result from differences in coating loss severity, which increases with cutting speed, and the adhesion of workpiece material layers. At lower cutting speeds (60 m/min), the coating remains largely intact, while higher cutting speeds cause more significant coating damage and greater exposure of the substrate.

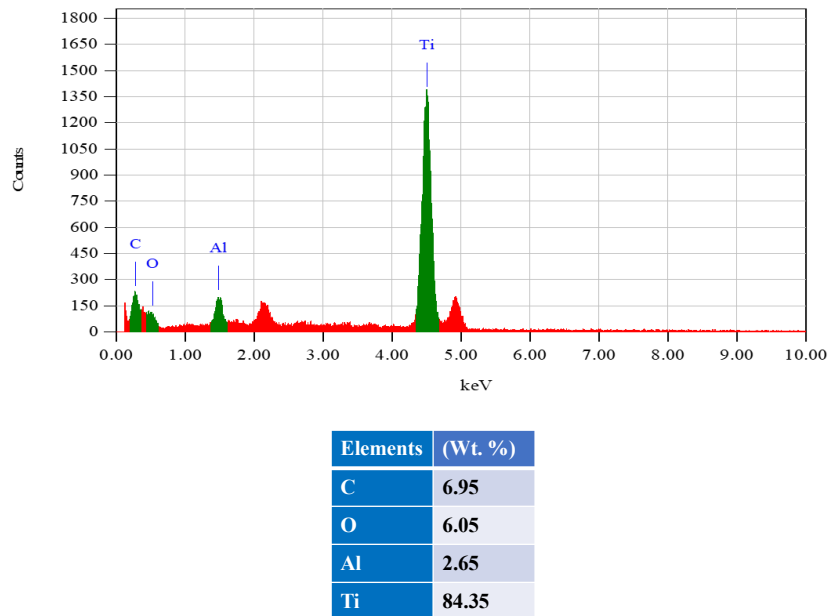


Fig. 17. EDS analysis of the fresh CVD-coated carbide insert before cutting

The wear mechanisms of the CVD-coated carbide inserts were examined by SEM after the experiments, and EDS spot analysis on the worn areas revealed that the dominant wear mechanisms evolved with increasing cutting speed, consistent with previous research on hard turning [33].

At cutting speed 60 m/min SEM images Fig. 18(a) revealed coating delamination and parallel abrasion marks on the flank, indicative of abrasive wear and formation of grooves caused by hard metallic carbides in the steels [15]. EDS analysis (Fig. 18(b)) confirmed strong Al and Ti peaks from the tool coating, suggesting the protective layer remained largely intact. Minor Fe traces indicated slight workpiece material adhesion, and low Oxygen content ruled out significant oxidation. Consequently, small scale abrasion with coating delamination dominated at low cutting speeds in hard turning, aligning with prior research [34].

At a cutting speed of 95 m/min, Fig. 19, SEM analysis revealed the formation of a built-up edge on the rake face, characteristic of adhesive wear during the hard turning [35]. EDS confirmed elevated Fe, Cr, and Ni transferred from the AISI 4340 workpiece. The progression of flank wear and repeated BUE, detachment indicates cyclic adhesion and tearing, corroborating existing research [36,37]. Although coating elements were still detected, at lower levels than at 60 m/min, indicating that the coating was not completely removed. Their reduced intensity indicated partial loss of the protective layer. adhesion and abrasion occur concurrently at this intermediate speed, with elevated temperatures accelerating material transfer.

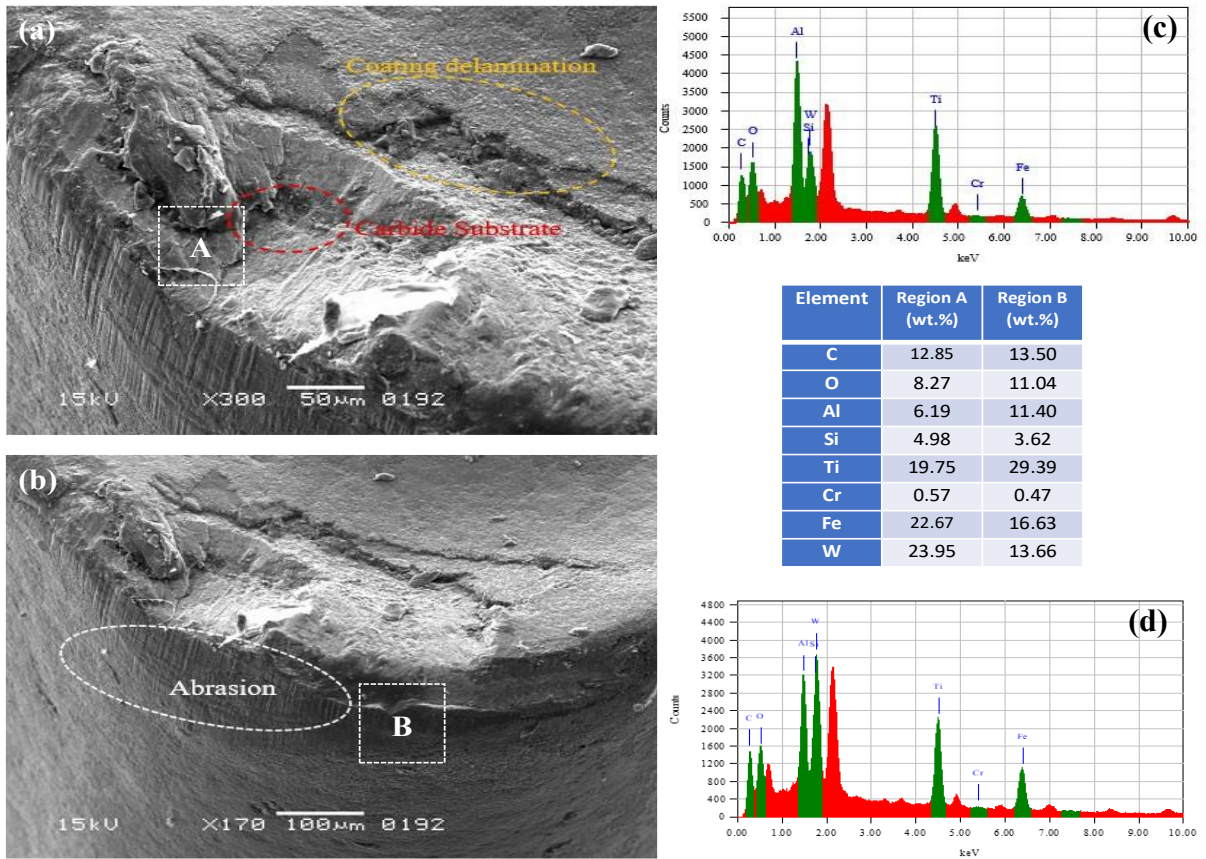


Fig. 18. SEM (a,b) and EDS (c,d) analysis on the worn tool at V = 60 m/min

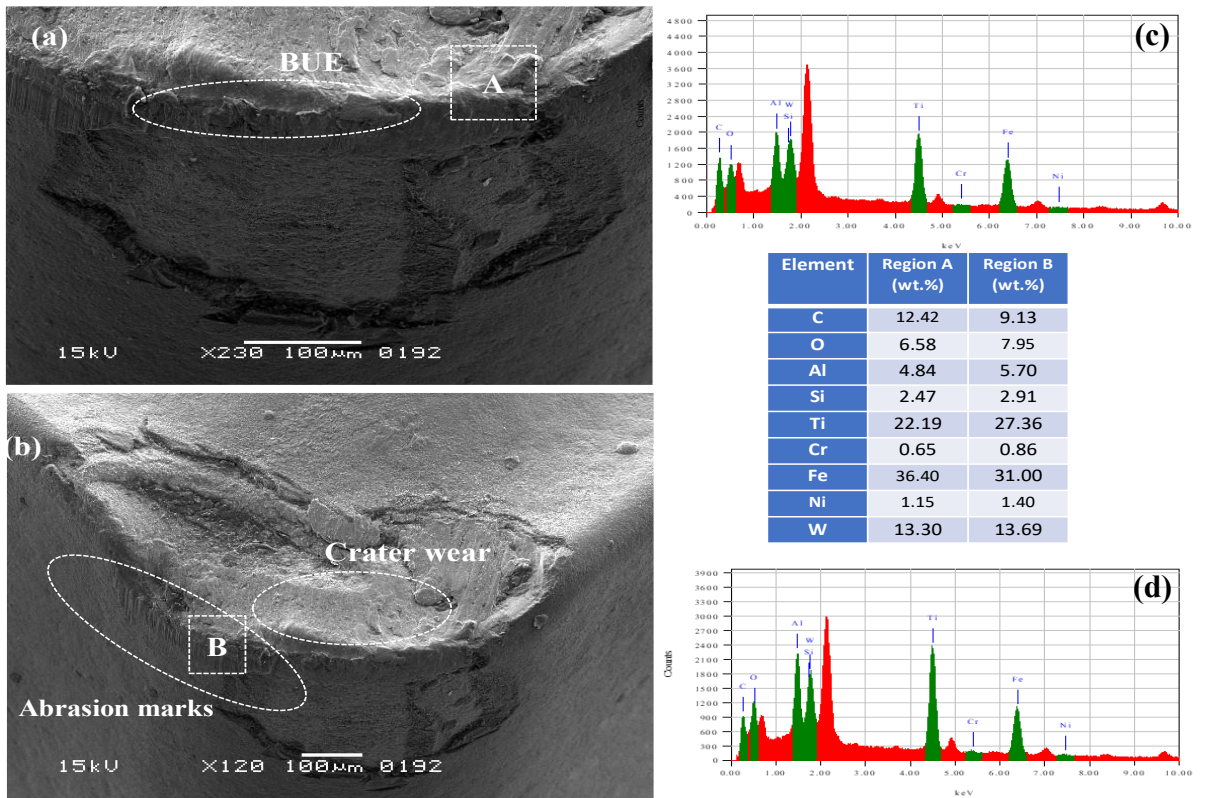


Fig. 19. SEM (a,b) and EDS analysis (c,d) on the worn tool at V = 95 m/min

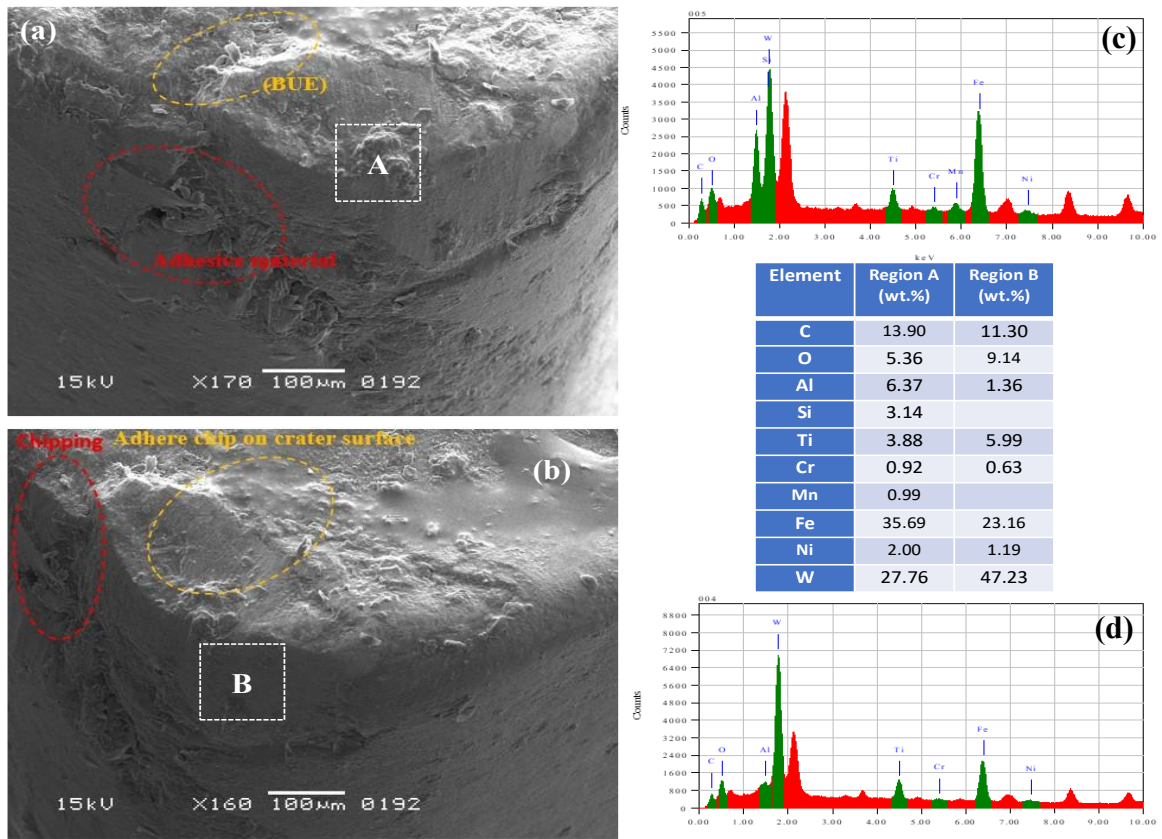


Fig. 20. SEM (a,b) and EDS analysis (c,d) on the worn tool at V = 180 m/min

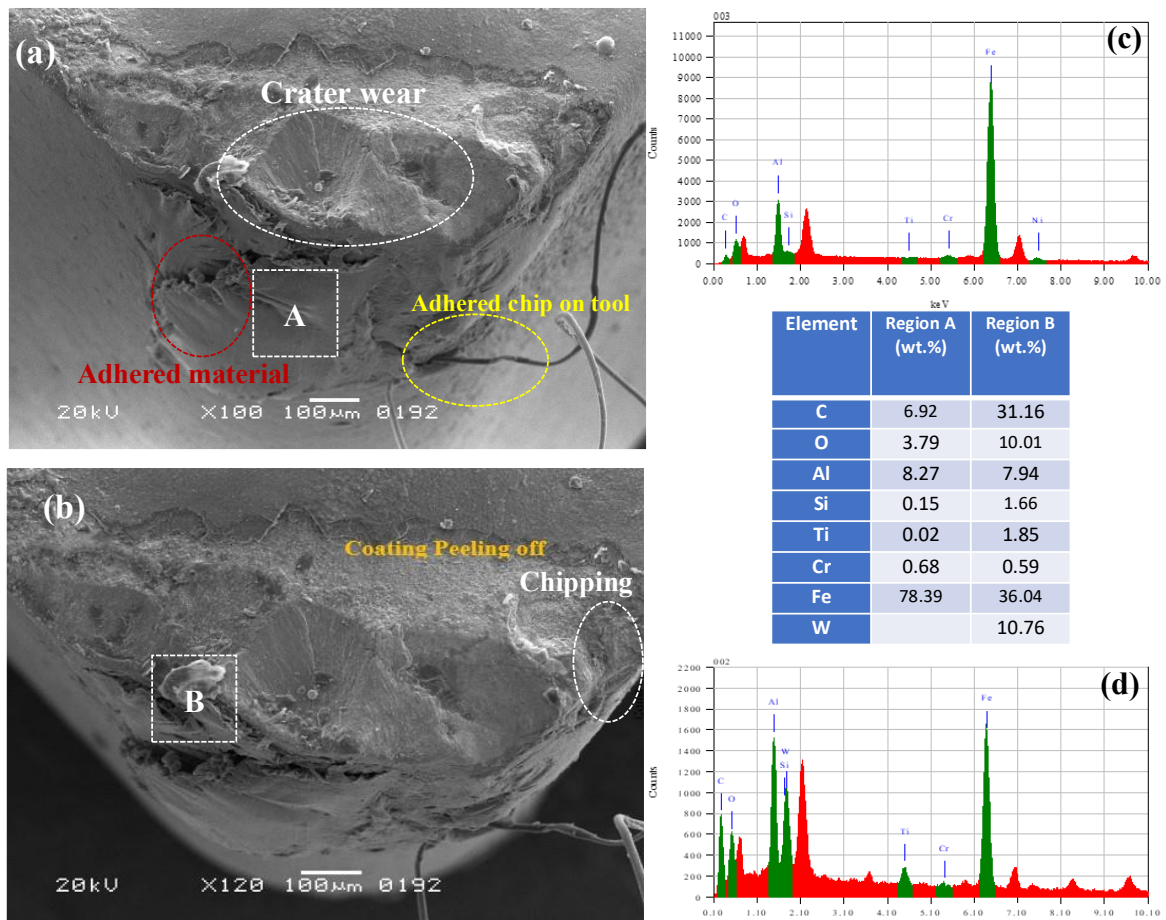


Fig. 21. SEM (a,b) and EDS analysis (c,d) on the worn tool at V = 250 m/min

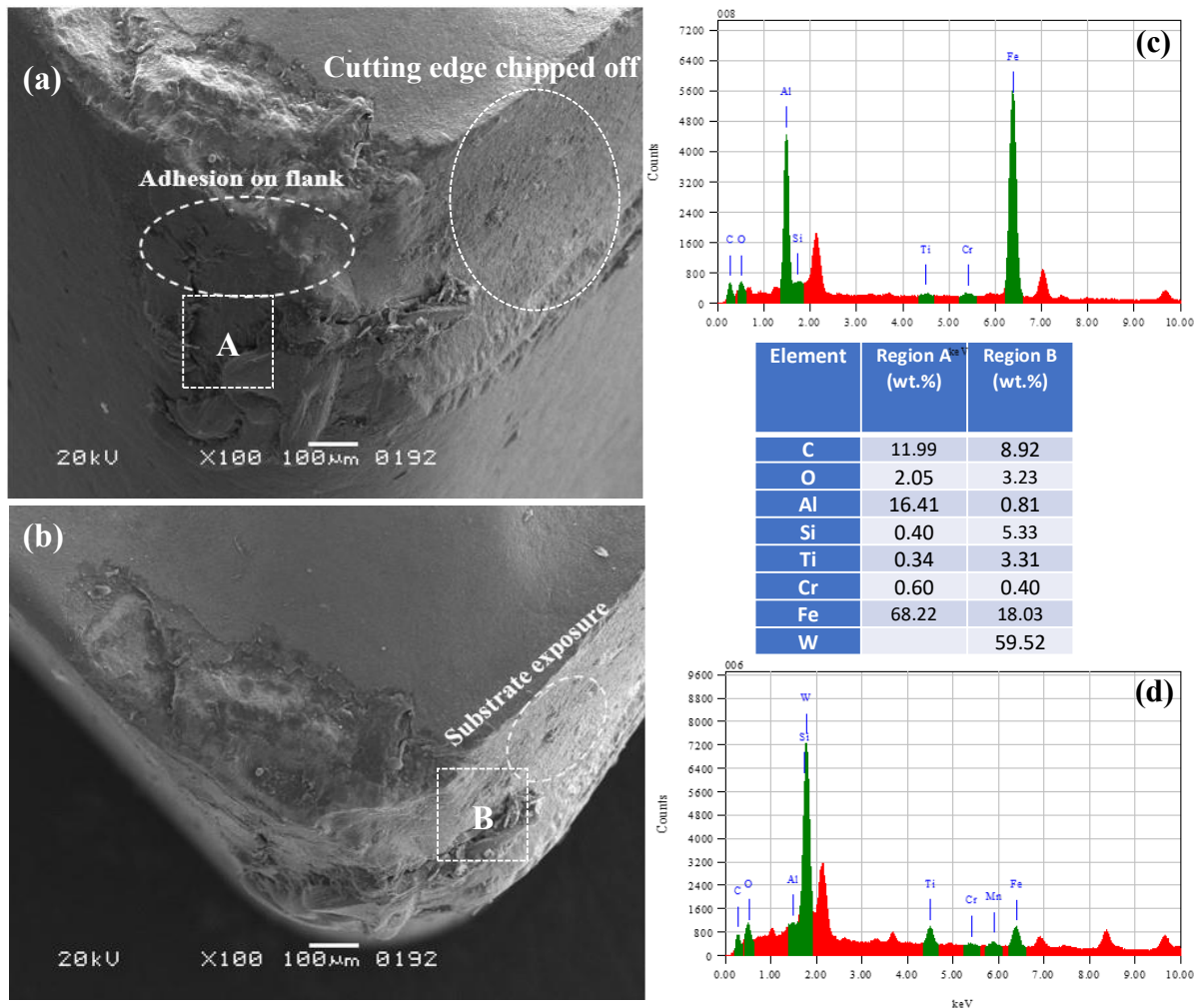


Fig. 22. SEM (a,b) and EDS analysis (c,d) on the worn tool at $V = 250$ m/min (wet)

Furthermore at 180 m/min, SEM images (Fig. 20) revealed crater formation on the rake face, pitting, and a pronounced flank wear land. EDS spectra showed a strong Fe peak and a distinct oxygen signal, suggesting adhesive oxidative wear. Reduced Al and Ti peaks, along with the appearance of W, indicated coating removal and exposure of the carbide substrate. These findings are consistent with reports of crater wear in hard turning, where adhesion, abrasion, and oxidation dominate at higher cutting speeds [18,38].

At a cutting speed of 250 m/min, SEM examination revealed significant tool degradation, characterized by deep cratering, edge fragmentation, and considerable plastic deformation at the tool-chip contact zone. EDS analysis presented in Fig. 21 indicated substantial adhesion and oxidation, as evidenced by elevated Fe and O signals, also deep crater formation on rake face of tool is evident. EDS indicates reduced coating elements and increased Fe and O consistent with coating loss and oxidation signify the failure of the protective coating and exposure of the underlying substrate shows flaking. Furthermore, SEM imaging Fig. 21 captured adhered chip fragments fused to the rake face, which are prone to dislodgment, leading to the removal of both coating and substrate material. This mode of wear is a recognized phenomenon in the high-speed hard turning of steels [36,39].

Interestingly, at 250 m/min (with coolant), tool wear was surprisingly more severe. Although oxidation appeared slightly reduced, SEM images (Fig. 22) revealed catastrophic


coating spallation, edge chipping, and substrate exposure. EDS spectra confirmed strong Fe peaks (workpiece adhesion) and W signs the exposure of substrate. These results reveals that conventional cutting fluids were ineffective at controlling the extremely high temperatures in high speed hard turning, leading instead to accelerated flaking and rapid tool failure [32,40].

Conclusions

In this work, CVD-coated carbide inserts TiCN/Al₂O₃ were used for high-speed hard turning of AISI 4340 steel. Tool wear, surface roughness, and the main wear mechanisms were examined under different cutting speeds and machining environments. From the study, the following points can be concluded:

1. Flank wear (VB) increased with cutting speed in a consistent manner. It went from about 186 µm at 60 m/min to 265 µm at 180 m/min, and then jumped sharply to 542 µm under dry cutting at 250 m/min. Under wet cutting at 250 m/min, tool wear reached 692 µm because of heavy flaking and fast coating delamination, which is well beyond the ISO 3685 tool life criterion (VB = 300 µm).
2. SEM and EDS analysis confirmed that at lower cutting speeds (60–95 m/min), light abrasive wear with mild coating delamination and small-scale abrasion were the main modes. At medium speed (around 180 m/min), adhesion and oxidation effects became more visible, and crater wear also appeared. At the highest tested speed (250 m/min), catastrophic tool failure occurred with severe coating spallation, edge chipping, strong adhesion, oxidation and exposure of the substrate at the tool edge.
3. Under flood-cooling condition, higher wear was observed at 250 m/min compared to dry cutting. SEM/EDS revealed increased spallation and adhered workpiece material, suggesting that coolant boiling and ineffective interface cooling may contribute to coating failure in this condition. Further testing with alternative cooling/lubrication strategies is required to confirm the generality of this observation.
4. The range 95 and 180 m/min is suitable cutting speed range for the machining of AISI 4340 steel under the present conditions. At this range, machining performance was found to be more consistent, with improved surface finishing and long tool life compared to both at very low and at very high speeds.
5. For future work, advanced cooling and lubrication methods such as minimum quantity lubrication (MQL) or cryogenic cooling will be investigated, as they could help reduce severe wear at higher speeds and increase tool life during hard turning.

CRedit authorship contribution statement

Murad Zulficar: conceptualization, methodology, investigation, formal analysis, data curation, writing – original draft, writing – review & editing; **Abdul Sattar Jamali**: conceptualization, supervision, writing – review & editing; **Saddam Hussain** : data curation.

Conflict of interest

The authors declare that they have no conflict of interest.

References

1. Barros RA, Abdalla AJ, Rodrigues HL, Pereira MDS. Caracterização de um aço AISI/SAE 4340 com diferentes microestruturas através da técnica de tríplex ataque. *Revista brasileira de aplicações de vácuo*. 2015;34(2): 71–74.
2. Sujitno T, Mulyani E, Suprpto, Andriyanti W, Suharlan D, Malau V. Effect of Diamond-Like Carbon Thin Film on the Fatigue Strength of AISI 4340 Steel. *Advances in Materials*. 2019;8(1): 21–26.
3. Wang L, Zhang Y, Liu H. Study on Experimental Method of Fracture Toughness for AISI 4340 Steel Using Circumferentially Cracked Round Bar. *SSRN*. [Preprint] 2025. Available from: <https://doi.org/10.2139/ssrn.5079339>
4. Kamruzzaman M, Dhar N. Effect of High-Pressure Coolant on Temperature, Chip, Force, Tool Wear, Tool Life and Surface Roughness in Turning AISI 1060 Steel. *Gazi University Journal of Science*. 2010;22(4): 359–370.
5. Boztepe A, Gecu R. Influence of Cryogenic Treatment and Tempering Temperature on Microstructural Evolution and Dry Sliding Wear Behavior of AISI D3 Cold-Work Tool Steel. *Journal of Tribology*. 2025;147(6): 064201.
6. Selvaraj DP. Optimization of surface roughness of duplex stainless steel in dry turning operation using Taguchi technique. *Materials Physics and Mechanics*. 2018;40(1): 63–70.
7. Darwish A. A Novel Deep Learning Model for Tool Wear Estimation of Cutting Tools. *Sustainable Machine Intelligence Journal*. 2024;9(1): 2.
8. Minquiz GM, González-Sierra NE, Méndez JF, Reyes ACP, Moreno MM, Morales-Sánchez A, López JAL, Hernandez-Simon ZJ, Carral CD. Analysis of Wear Mechanisms Under Cutting Parameters: Influence of Double Layer TiAlN/TiN PVD and TiCN/Al₂O₃ Chemical Vapor Deposition-Coated Tools on Milling of AISI D2 Steel. *Coatings*. 2024;14(12): 1491.
9. Calaph YC, Ganesh PSPS, Shanawaz AM, Kavitha S, Muthusamy C, Arunprasath K. Analysing the impact of cutting parameters of CNC machining on EN8 steel with high strength carbide tool tip insert. *Interactions*. 2024;245: 74.
10. Šramhauser K, Kraus P, Špalek F, Černý P, Ufetikirezi JDDM, Zoubek T, Strob M, Kononets Y, Kříž P, Vochozka V. Intercomparison of Indexable Cutting Inserts' Wear Progress and Chip Formation During Machining Hardened Steel AISI 4337 and Austenitic Stainless Steel AISI 316 L. *Materials*. 2024;17(22): 5418.
11. Bag R, Panda A, Sahoo AK, Kumar R. Sustainable High-Speed Hard Machining of AISI 4340 Steel Under Dry Environment. *Arabian Journal for Science and Engineering*. 2023;48: 3073–3096.
12. Najar K, Mursaleen M, Dar T. Experimental evaluation of multilayered CVD- and PVD-coated carbide turning inserts in severe machining of AISI-4340 steel alloy. *Jurnal Tribologi*. 2021;29: 117–143.
13. Kishore G, Parthiban A, Mohana Krishnan A, Radha Krishnan B. Investigation of the surface roughness of aluminium composite in the drilling process. *Materials Physics and Mechanics*. 2021;47(5): 739–746.
14. Khurtasenko AV, Cherednikov II, Mamchenkova AA, Chauev KV, Bondarenko AA. Assessment of wear and destruction of solid carbide cutters during milling of hardened steel 4X5MF1C with a hardness of 52 HRC. *Bulletin of BSTU named after V.G. Shukhov*. 2024;6: 81–92.
15. Hassan S, Khan SA, Naveed R, Saleem MQ, Mufti NA, Farooq MU. Investigation on tool wear mechanisms and machining tribology of hardened DC53 steel through modified CBN tooling geometry in hard turning. *The International Journal of Advanced Manufacturing Technology*. 2023;127(1–2): 547–564.
16. Santos AJD, Reis BCM, Pereira NFS, De Oliveira DA, Rubio JCC, Abrão AM, Câmara MA. Tribological effects of micromilling of hardened AISI D2 steel on tool wear and top burr formation. *The International Journal of Advanced Manufacturing Technology*. 2023;127: 5327–5341.
17. Ahmed F, Kumaran ST, Ahmad F. Analysis of Wear Mechanisms and Chip Morphology During Machining of Tool Steel Using TiAlSiCrN-Coated WC-Co Ball end Mills. To be published in *Research Square*. [Preprint] Available from: doi.org/10.21203/rs.3.rs-1144076/v1
18. Jouini N, Yaqoob S, Ghani JA. Investigations on the machinability performance of Al₂O₃/TiCN CVD coated carbide tools in sustainable high-speed hard-turning of AISI 4340 alloy steel. *Materials Research Express*. 2024;11(9): 096509.
19. Silva RYOAD, Silva MLD, Conti PHDMC, Costa AFD. Application of CVD Coated Turning Inserts in the Machining of ABNT 8620 Steel at Different Cutting Speeds. *Revista De Gestão Social E Ambiental – RGSA*. 2024;18(12): e010133.
20. Cakan A, Albayrak O, Gozmen Sanli B, Guven O, Ugurlu M, Atmaca H. Cutting performance of coated carbide inserts in hard turning of hardened AISI D2 cold work tool steels. *Proceedings of the Institution of Mechanical Engineers, Part C: Journal of Mechanical Engineering Science*. 2024;238(19): 9504–9513.
21. Rashid WB, Goel S, Davim JP, Joshi SN. Parametric design optimization of hard turning of AISI 4340 steel (69 HRC). *The International Journal of Advanced Manufacturing Technology*. 2016;82: 451–462.
22. Kumar R, Sahoo AK, Mishra PC, Das RK. Comparative study on machinability improvement in hard turning using coated and uncoated carbide inserts: part II modeling, multi-response optimization, tool life, and economic aspects. *Advances in Manufacturing*. 2018;6: 155–175.

23. Hamadi B, Yallese MA, Boulanouar L, Khellaf A, Haddad A. A Comparative Study of the Performance of Uncoated, PVD, CVD and MTCVD Coated Carbide Inserts in Dry Turning of AISI4140 Steel. *Periodica Polytechnica Mechanical Engineering*. 2022;66(4): 314–324.
24. Pawan S, Gupta K. Dry Machining Techniques for Sustainability in Metal Cutting: A Review. *Processes*. 2024;12(2): 417.
25. Panda A, Sahoo AK, Panigrahi I, Kumar R. Tool condition monitoring during hard turning of AISI 52100 Steel: A case study. *Materials Today: Proceedings*. 2018;5(9): 18585–18592.
26. Bushlya V, Gutnichenko O, Zhou J, Avdovic P, Ståhl J-E. Effects of cutting speed when turning age hardened Inconel 718 with PCBN tools of binderless and low-CBN grades. *Machining Science and Technology*. 2013;17(4): 497–523.
27. Mitsubishi Materials Corporation. *Turning inserts: CNMG120404-MA*. Available from: https://www.mitsubishicarbide.net/mht/enuk/turning_inserts/no_srs/20041777 [Accessed 22th September 2025]
28. Novakova J, Petrkovska L, Brychta J, Cep R, Ocnasova L. Influence of high speed parameters on the quality of machined surface. *World Academy of Science, Engineering and Technology*. 2009;56: 274–277.
29. Miko E, Nowakowski Ł. Analysis and Verification of Surface Roughness Constitution Model After Machining Process. *Procedia Engineering*. 2012;39: 395–404.
30. Nouari M, List G, Girot F, Coupard D. Experimental analysis and optimisation of tool wear in dry machining of aluminium alloys. *Wear*. 2003;255(7–12): 1359–1368.
31. Sharma VS, Dogra M, Suri NM. Cooling techniques for improved productivity in turning. *International Journal of Machine Tools and Manufacture*. 2009;49(6): 435–453.
32. Dhar N, Kamruzzaman M. Cutting temperature, tool wear, surface roughness and dimensional deviation in turning AISI-4037 steel under cryogenic condition. *International Journal of Machine Tools and Manufacture*. 2007;47(5): 754–759.
33. Mallick R, Kumar R, Panda A, Sahoo AK. Current Status of Hard Turning in Manufacturing: Aspects of Cooling Strategy and Sustainability. *Lubricants*. 2023;11(3): 108.
34. Cakan A. Wear behavior of multilayer coated carbide tools in finish dry hard turning. *Materials Testing*. 2016;58(9): 772–777.
35. Szablewski P, Legutko S, Ungureanu N, Petru J, Smak K, Krawczyk B. Comparative Assessment of Tool Wear and Surface Topography After Superfinish Turning of Inconel 718 with Carbide and Ceramic Inserts. *Applied Sciences*. 2025;15(8): 4265.
36. Ranjan Das S, Panda A, Dhupal D. Hard turning of AISI 4340 steel using coated carbide insert: Surface roughness, tool wear, chip morphology and cost estimation. *Materials Today: Proceedings*. 2018;5(2): 6560–6569.
37. Wagri NK, Jain NK, Petare A, Das SR, Tharwan MY, Alansari A, Alqahtani B, Fattouh M, Elsheikh A. Investigation on the Performance of Coated Carbide Tool during Dry Turning of AISI 4340 Alloy Steel. *Materials*. 2023;16(2): 668.
38. Yaqoob S, Ghani JA, Jouini N, Juri AZ. Performance evaluation of PVD and CVD multilayer-coated tools in machining high-strength steel. *Coatings*. 2024;14(7): 865.
39. Chinchankar S, Choudhury SK. Wear behaviors of single-layer and multi-layer coated carbide inserts in high speed machining of hardened AISI 4340 steel. *Journal of Mechanical Science and Technology*. 2013;27: 1451–1459.
40. Jasni NAH, Lajis MA, Kamdani K. Tool Wear Performance of TiAlN/AlCrN Multilayer Coated Carbide Tool in Machining of AISI D2 Hardened Steel. *Advanced Materials Research*. 2012;488–489: 462–467.